ELSEVIER

Physica C 353 (2001) 5–10

PHYSICA C

www.elsevier.nl/locate/physc

Synthesis and processing of MgB_2 powders and wires

C.E. Cunningham [1], C. Petrovic, G. Lapertot [2], S.L. Bud'ko, F. Laabs, W. Straszheim, D.K. Finnemore *, P.C. Canfield

Ames Laboratory, US Department of Energy and Department of Physics and Astronomy, Iowa State University, Ames, IA 50011, USA

Received 12 March 2001; accepted 19 March 2001

Abstract

Sintered powders and wires of superconducting MgB_2 have been fabricated under a variety of conditions in order to determine details of the diffusion of the Mg into B and to study the types of defects that arise during growth. For samples prepared by exposure of boron to Mg vapor at 950°C, the conversion of particles of less than 100 μm size to MgB_2 is complete in about 2 h. The lattice parameters of the MgB_2 phase determined from X-ray are independent of the starting stoichiometry and the time of reaction. Wire segments of MgB_2 with very little porosity have been produced by reacting 141 μm diameter boron fibers in an atmosphere of excess Mg vapor at 950°C. Defects in the reacted fibers are predominantly voids left as the boron is converted to MgB_2. Published by Elsevier Science B.V.

Keywords: MgB_2 powder; MgB_2 wire; Synthesis

1. Introduction

The discovery of superconductivity in the intermetallic compound, MgB_2 near 40 K [1] has prompted both fundamental studies of the mechanism causing superconductivity [2] and practical studies of supercurrent transport at grain boundaries [3,4]. Bud'ko and co-workers [2] have shown the existence of a boron isotope effect in that $T_c \sim M^{\alpha}$ with $\alpha = 0.26$, where T_c is the superconducting transition temperature and M is the isotopic mass. This result implies that the electron–phonon interaction is important in the determination of T_c and that light elements with high phonon frequencies might be important in the search for new metallic superconductors with high transition temperatures. Energy gap measurements [5,6] and neutron scattering measurements of the phonon spectrum [7] all point to a conventional mechanism for the superconductivity. On the practical side, Canfield and co-workers [8] have shown a method to convert commercially available boron fibers [3] into very low resistivity MgB_2 wire and Takano and co-workers [9] have measured the current carrying capacity of hot-pressed pellets of the material. Other measurements of flux pinning

* Corresponding author. Tel.: +1-515-294-3455; fax: +1-515-294-0689.

E-mail address: finnemor@ameslab.gov (D.K. Finnemore).

[1] On leave from Department of Physics, Grinnell College, Grinnell, IA 50112, USA.

[2] On leave from Commissariat a l'Energie Atomique DRFMC-SPSMS, 38054 Grenoble, France.

[3] Textron Systems, 201 Lowell Street, Wilmington, MA 01887.

0921-4534/01/$ - see front matter Published by Elsevier Science B.V.
PII: S0921-4534(01)00397-5

and intergrain coupling have been made using studies of flux creep [10].

In this paper, we report a systematic study of the vapor diffusion method of sample preparation for both microcrystalline powders and boron (B) fibers, which are available commercially in kilometer lengths. The primary variable in the study is time, and for the wire samples the effect of defects in the starting B fibers. Of particular interest is the role of the tungsten-boride core in creating cracks and transmitting Mg along the length of the fiber.

2. Experiment

For powder synthesis, we place a stoichiometric mixture of bright lumps of Mg (99.9%) and fine crystalline ^{11}B powder (99.5%) that is less than 100 μm in diameter into a Ta tube whose ends are sealed under a partial atmosphere of Ar. For the wire synthesis, we cut B fiber lengths several cm long and either 100 or 141 μm in diameter and place them in Ta tubes under a partial pressure of Ar with excess Mg. These starting B fibers have a tungsten-boride core about 15 μm in diameter with breaks every few cm.

After the Ta tubes are sealed, they are in turn sealed in quartz ampoules with ~175 mbar of Ar and placed in a box furnace preheated to 950°C. It is believed that using a preheated furnace inhibits the growth of higher boron phases. After reaction, the samples are rapidly cooled by putting the quartz tube in running cold water. The formation of MgB_2 from B causes the powders to expand and bow the Ta tube outward [2] and causes 100 μm diameter wires to expand by more than 30% in diameter [8].

Samples are characterized by X-ray diffraction, magnetization, and electrical resistivity. X-ray diffraction spectra are taken with Cu K_α radiation in a Scintag diffractometer where the scan angle 2θ varies from 20° to 90° with a scan step of 0.020°. Magnetization is measured in a Quantum Design MPMS-5 magnetometer with a 6 cm sample travel in a magnetic field of 25 Oe in a zero-field-cooled mode. Resistivity is measured with a standard four probe technique using an LR-700 resistance bridge.

3. Results and discussion

The lattice constants of the MgB_2 phase, determined from X-ray data, change relatively little with time of reaction for powders and have values close to those previously reported [11]. The dynamics of the growth of the MgB_2 phase are illustrated by the study of powder diffraction X-ray data after different times of reaction in Fig. 1. The major B peak at 38°, marked by the solid line on the figure, is small and goes away during processing. For particle sizes used here (less than 100 μm), the MgB_2 peaks grow quickly between 30 min and 60 min and remain relatively unchanged from 120 to 240 min. The Si peaks used for a standard have been removed from these spectra. It should be noted that when the reaction ampoule was placed in a furnace, heated to 950°C, left for 120 min, and quenched, the powder X-ray spectra showed many second phase peaks. Zero-field-cooled magnetization measurements for these same samples show the transition width narrowing from 15 to 30 min and then remaining relatively constant at about 0.5 K.

Electrical resistivity of the sintered pellets is compared to the wires in Fig. 2. The inset in Fig. 2 shows an expanded view near the transition temperature and indicates values at 40 K of about 1.5 μΩ cm for the pellets and 0.4 μΩ cm for the wire segments. These processing methods give very low

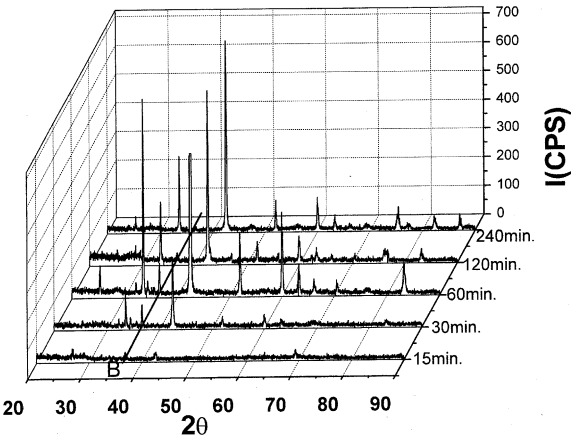

Fig. 1. X-ray spectra for boron powder reacted for different times.

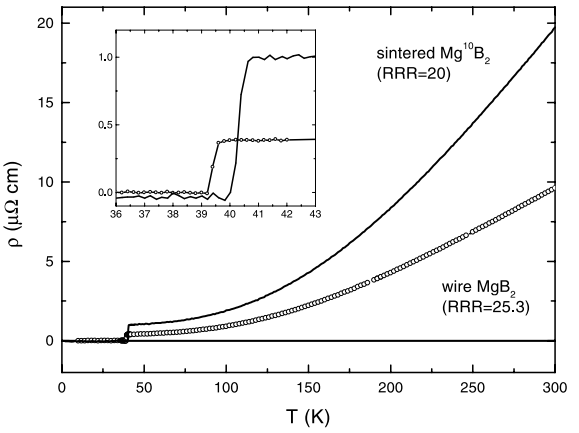

Fig. 2. Comparison of electrical resistivity of a sintered pellet and a reacted wire segment.

electrical resistivity in the normal state for both pellets and wires. Because both the relatively open structure of the pellet and the dense structure of the wire samples have comparable residual resistivity ratios, RRR $\geqslant 20$, we think the lower resistivity values for the wire sample are due to its higher density.

In order to study the synthesis of MgB_2 wire, a series of exposure time, t, of the boron fibers in Mg vapor was measured for $15 \leqslant t \leqslant 240$ min. For the processing of the 100 μm diameter fibers, the scanning electron micrographs in Fig. 3a and b illustrate the behavior seen. In these micrographs, Mg has a much higher atomic number than B so the shading is a good indication of Mg content. In Fig. 3a, a length of fiber reacted for 60 min has been polished through a section that misses the tungsten-boride core in the middle of the fiber. The Mg concentration is very high at the outside surface region marked (1), and there is a clear front of Mg moving across the fiber. At the boundary between the regions marked (2) and (3), energy dispersive X-ray spectra (EDS) show that the Mg level abruptly falls by about 40%. Region (3) has a fairly high Mg content, even though it has not transformed to the MgB_2 phase. As shown by the diameter lines, the diameter of this section has grown by more than 10% from the original 100 μm.

A different section of fiber reacted for 60 min in the same run as in Fig. 3a is shown in Fig. 3b. Here the polishing just barely exposes the tungsten-boride core along the centerline. This SEM micrograph shows many of the common defects. The dark line along the center is a void region, which often occurs near the tungsten-boride core, and an EDS spectrum shows very strong W lines in this region. The bright region marked (A) is an MgB_2 region and the dark region marked (B) is a Mg deficient region. If optical pictures are taken, the B regions stand up above the MgB_2 regions because they are harder and polish less rapidly.

Fig. 3c shows an EDS line scan measurement of the Mg concentration taken along the light line running from upper left to lower right in the left-center portion of Fig. 3b. The Mg count on Fig. 3c drops from about 1.4 to about 0.9 going from the bright region to the dark region. The tick mark on the line in Fig. 3b corresponds to the vertical line in Fig. 3c and to a point where the scan moves from a dark region back into a bright region near the core. Magnesium seems to diffuse very rapidly along the core region and diffuse outward from there to form MgB_2. The void region shown by the dark area in the upper left corner of Fig. 3b is unusually large, and the bottom of the void is clearly seen in the SEM. Voids are commonly about 10–20 μm across, and the bottom of the void generally can be seen in the SEM. The diagonal regions of high Mg content we believe are cracks where the Mg can diffuse rapidly and start the formation of MgB_2.

A B fiber reacted for 30 min is shown in Fig. 4a. Again the polishing depth does not cut through the core. The sample has much less conversion to MgB_2, shown by the bright spots. EDS measurements show the highest Mg content in the bright spot marked (C), substantially less Mg near the edge at the point marked (A), and even less at the point near the center marked (B).

Another B fiber reacted for 15 min is shown in Fig. 4b. In the left edge of this fiber, the tungsten core shows through, and the diameter of the fiber is still close to 100 μm. The EDS data show only a small amount of Mg near the edge of the fiber and practically none in the center of the fiber.

When exposure time, $t = 120$ min, the 100 μm starting diameter fibers are fully reacted and end

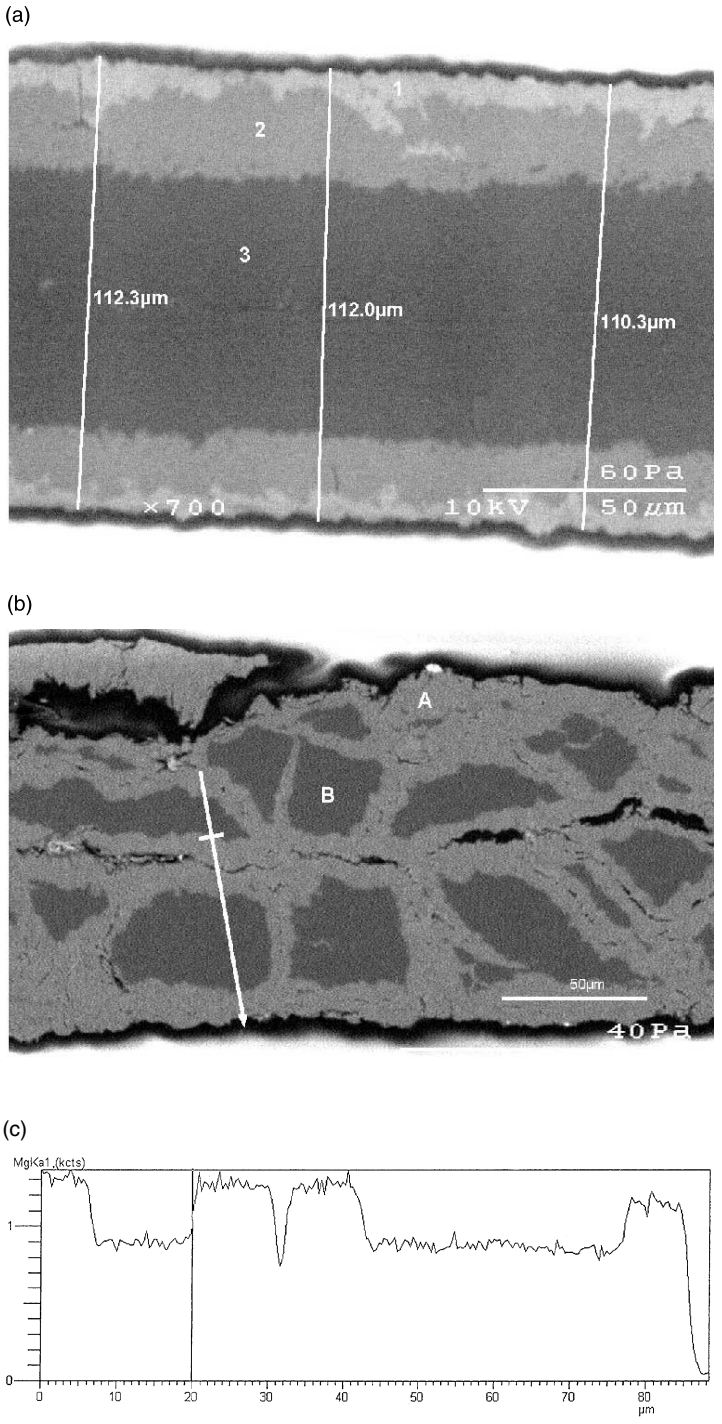

Fig. 3. SEM micrograph of two segments of 100 μm diameter boron fibers after 60 min in Mg vapor at 950°C: (a) is an EDS scan along the line drawn in (b).

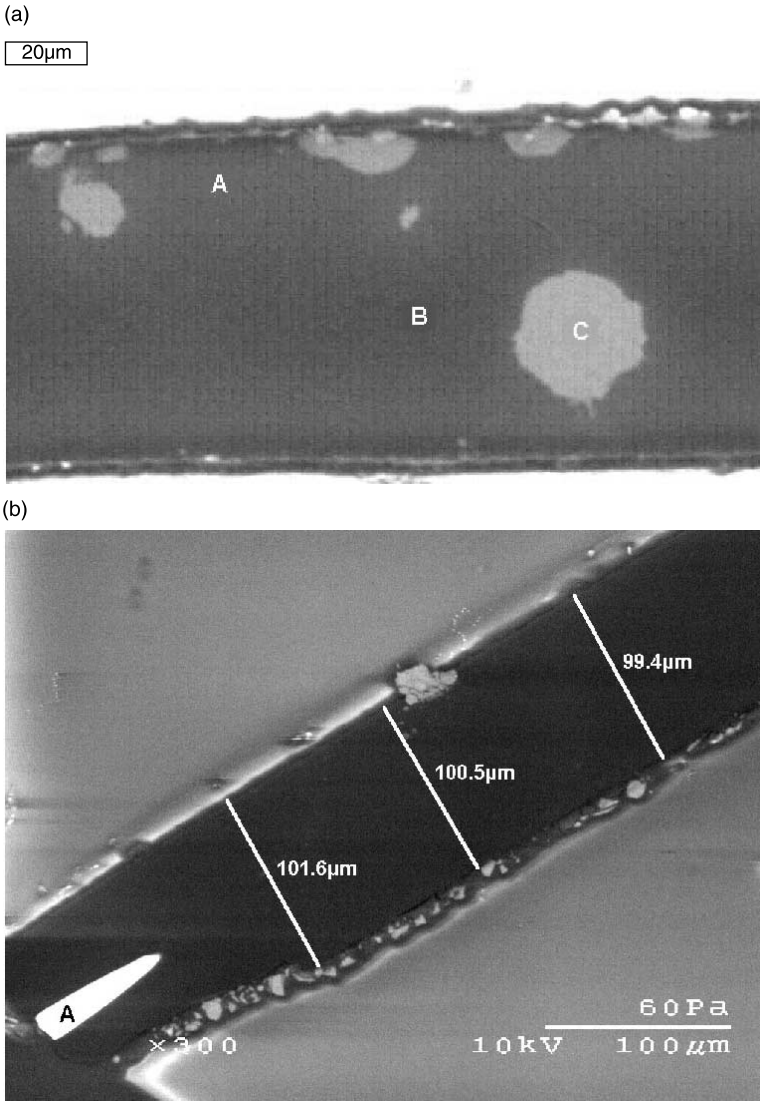

Fig. 4. SEM micrographs of 100 μm boron fibers reacted for (a) 30 min and (b) 15 min.

up having a final diameter of about 160 μm. To examine how the process scales with initial fiber size, a 141 μm diameter fiber was exposed for a much longer time, $t = 36$ h, with the results shown in Fig. 5. The conversion to MgB_2 has increased the diameter of the wire to greater than 180 μm, as shown by the diameter measurements. There are no second phase particles large enough to be seen in the SEM micrograph, and the fiber is relatively void free.

4. Conclusions

Low resistivity, high purity powders and dense wires of MgB_2 can be synthesized by exposure of boron powder and boron fibers to Mg vapor at 950°C for adequate exposure time. Comparable results are seen for both 100 and 141 μm diameter fibers. For 100 μm B fibers that are placed in a furnace preheated to 950°C, the MgB_2 phase begins to form quickly after about 15 min and is

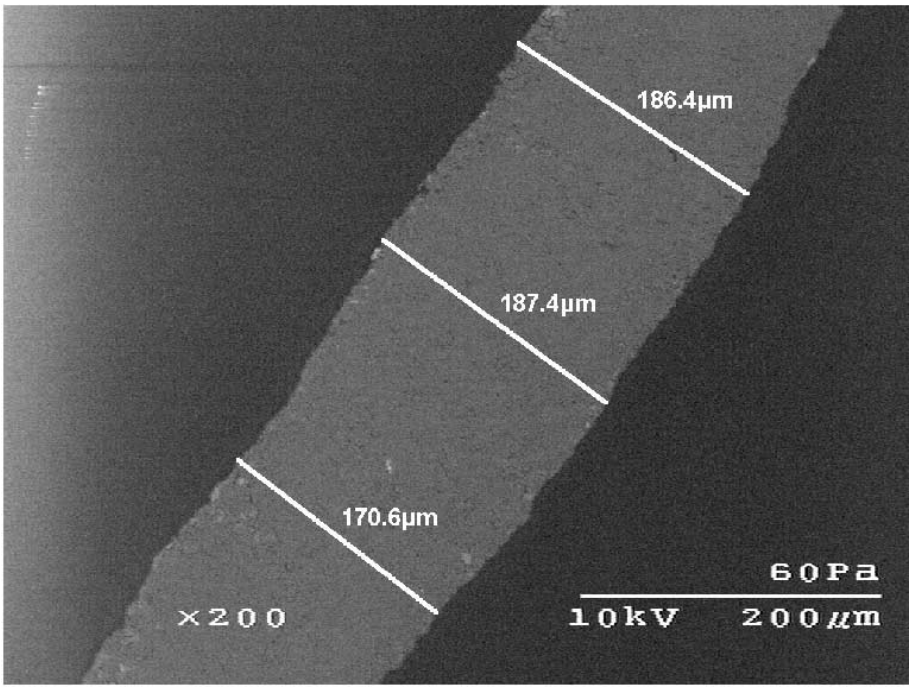

Fig. 5. SEM micrographs of a wire segment for the larger diameter boron fiber that is fully reacted.

about 50% complete after an hour. Diffusion of Mg along the tungsten-boride core and along voids or cracks in the fiber are important means of transport. As the MgB_2 phase forms, the diameter of the fiber grows from about 141 to about 190 μm. As reported earlier [8], the wire segments provide a highly conducting material with a normal state resistivity of about 0.4 μΩcm and a superconducting critical current density of about 20,000 A/cm^2 at 1 T and 20 K.

Acknowledgements

Work is supported by the US Department of Energy, Basic Energy Sciences, Office of Science, through the Ames Laboratory under Contract no. W-7405-Eng-82.

References

[1] J. Nagamatsu, N. Nakagawa, T. Muranaka, Y. Sentani, J. Akimitsu, Nature 410 (2001) 63.
[2] S.L. Bud'ko, G. Lapertot, C. Petrovic, C.E. Cunningham, N. Anderson, P.C. Canfield, Phys. Rev. Lett. 86 (2001) 1877.
[3] D.K. Finnemore, J.E. Ostenson, S.L. Bud'ko, G. Lapertot, P.C. Canfield, Phys. Rev. Lett. 86 (2001) 2420.
[4] D.C. Larbalestier, M. Rikel, L.D. Cooley, A.A. Polyanskii, J.Y. Jinang, S. Patnaik, X.Y. Cai, D.M. Feldmann, A. Gurevich, A.A. Squitier, M.T. Naus, C.B. Eom, E.E. Hellstrom, R.J. Cava, K.A. Regan, N. Rogado, M.A. Hayward, T. He, J.S. Slusky, K. Inumaru, M. Haas, Nature 410 (2001) 186.
[5] G. Karapetrov, M. Iavarone, W.K. Kwok, G.W. Crabtree, D.G. Hinks, cond-mat/0102312.
[6] H. Schmidt, J.F. Zasadzinski, K.E. Gray, D.G. Hinks, cond-mat/0102389.
[7] R. Osborn, E.A. Goremyshkin, A.I. Kolesnikov, D.G. Hinks, cond-mat/0103064.
[8] P.C. Canfield, D.K. Finnemore, S.L. Bud'ko, J.E. Ostenson, G. Lapertot, C.E. Cunningham, C. Petrovic, Phys. Rev. Lett. 86 (2001) 2423.
[9] Y. Takano, H. Takeya, H. Fujii, H. Kumakura, K. Togano, H. Kito, H. Ihara, cond-mat/0102167.
[10] Y. Bugoslavsky, G.K. Perkins, X. Qi, L.F. Cohen, A.D. Caplin, Nature 410 (2001) 563.
[11] N.V. Vekshina, L.Ya. Markovskii, Yu.D. Kondraschev, T.K. Voevodskaya, Zhurnal Prikladnoi Khimii 44 (1971) 970.